Viscoelasticity of Concentrated Isotropic Solutions of Semiflexible Polymers. 3. Nonlinear Rheology

David C. Morse

Department of Chemical Engineering and Materials Science, University of Minnesota, 421 Washington Avenue S.E., Minneapolis, Minnesota 55455

Received April 7, 1997; Revised Manuscript Received June 1, 1999

ABSTRACT: Nonlinear rheological properties of a tightly-entangled solution of persistent macromolecules are calculated within the context of a tube model. It is shown that the curvature stress in highly deformed solutions of such chains is dominated by the contributions of deformation-induced "hairpins", i.e., rare but very tightly curved segments of the deformed chain conformations. The model is found to exhibit strain softening in shear deformations.

I. Introduction

In two preceding papers,[1,2] hereafter referred to as (I) and (II), we introduced a tube model for tightly-entangled solutions of semiflexible polymers, i.e., solutions in which each polymer is effectively confined to a tube of diameter much less than the polymer persistence length. Here, we consider the nonlinear rheological response of the same model.

We will express the stress here, as in (II), as a sum of intramolecular curvature, orientational, and stress contributions and thus ignore any direct intermolecular (e.g., excluded volume) contributions to the stress. We focus in what follows primarily upon describing the more slowly decaying curvature and orientational stress contributions, which are expected to dominate the stress in all flow histories except those involving very rapid deformation. The model used here to describe stress relaxation is patterned rather closely on the original Doi−Edwards (DE) tube model[3,4] and shares with the DE model several defects that have been corrected in subsequent theoretical work on entangled flexible polymers. Specifically, (i) the primitive chain is taken to be completely inextensible, thus neglecting any diffusive or flow-induced changes in the contour length density of the primitive chain,[5−9] and (ii) the curvature stress is assumed to relax by simple reptation, thus neglecting any relaxation arising from either diffusive[10−12] or convective.[13,14] constraint release mechanisms. The most important difference between the present model and the DE model is the replacement of the freely jointed primitive chain of the DE model by a worm-like primitive chain. To focus attention first on the rheological consequences of this difference, we first compare the predictions of the present model to those of the original DE model and defer discussion of the expected limitations of the model to a separate section.

The paper is organized as follows: section II contains a calculation of the curvature stress induced by a step deformation of a solution of long coil-like polymers. Section III contains more qualitative discussion of the behavior of solutions of coil-like and rod-like polymers in continuous flow histories. Section IV is a discussion of some expected limitations of the model. Section V is summary of conclusions. All notation is the same as in (I) and (II). We refer to equations in these papers by prepending Roman numerals to the equation numbers; e.g., eq II.3 is eq 3 in (II).

II. Step Deformations

We first consider the stress induced by a large step deformation at time $t = 0$ by a total deformation tensor $\mathbf{E}$, for which macroscopic material elements are displaced as $\mathbf{r} \rightarrow \mathbf{E}\cdot\mathbf{r}$. We focus, for simplicity, on solutions of coil-like chains, with $L \gg L_p$, for which we may ignore the orientational contribution to the stress. The stress $\boldsymbol{\sigma}(t, \mathbf{E})$ at times $t > 0$ may thus be approximated as a sum

$$\boldsymbol{\sigma}(t, \mathbf{E}) \simeq \boldsymbol{\sigma}_{\text{tens}}(t, \mathbf{E}) + \boldsymbol{\sigma}_{\text{curve}}(t, \mathbf{E}) \qquad (1)$$

of a tension stress and a curvature stress.

As in the case of infinitesimal step deformations considered in (II), the tension stress is expected to be larger at early times but to decay much more rapidly than the curvature stress. Simple considerations, first mentioned by MacKintosh et al.,[15] suggest that the tension stress contribution will be strongly strain hardening: The microscopic tension in a segment of the primitive chain is expected to increase rapidly with the degree of tangential extension and to diverge as the end-to-end distance of the segment approaches the full contour length of the subchain, presumably leading to a correspondingly rapid increase in $\boldsymbol{\sigma}_{\text{tens}}(0, \mathbf{E})$ with increasing strain amplitude. It is, however, difficult to go much beyond such qualitative statements about the nonlinear behavior of $\boldsymbol{\sigma}_{\text{tens}}$, due to the mathematical difficulty of describing either the initial state of tension induced by a general step deformation or the subsequent relaxation process, except in the case of infinitesimal deformations (i.e., linear viscoelastic response) that is discussed in (II). In what follows, we focus instead upon calculating the more slowly decaying curvature stress $\boldsymbol{\sigma}_{\text{curve}}(t, \mathbf{E})$, because it is expected to dominate the total stress at all but very early times t and because its qualitative behavior is both harder to guess and (as it turns out) easier to calculate than that of the tension stress.

The time-dependence of $\boldsymbol{\sigma}_{\text{curve}}(t, \mathbf{E})$ is the same as that obtained in (II) for the case of an infinitesimal step

10.1021/ma970475j CCC: $18.00
Published on Web 08/10/1999

deformation and may be written as a product

$$\boldsymbol{\sigma}_{\text{curve}}(t, \mathbf{E}) = \boldsymbol{\sigma}_{\text{curve}}(\mathbf{E})\bar{\chi}(t) \tag{2}$$

In the above, $\boldsymbol{\sigma}_{\text{curve}}(\mathbf{E}) \equiv \boldsymbol{\sigma}_{\text{curve}}(0, \mathbf{E})$ is the curvature stress obtained immediately after the deformation, and $\bar{\chi}(t)$ is the relaxation function given in eq II.56. This relaxation function is the same as that used in the DE model[3] and is given physically by the probability that a section of tube chosen randomly at $t = 0$ will survive until time t.

In describing the deformation of the primitive chain of a specified polymer, the conformation of the chain just before the step deformations will be specified by a position $\mathbf{r}(s)$, with a unit tangent vector $\mathbf{u}(s) = \mathrm{d}\mathbf{r}(s)/\mathrm{d}s$ and curvature $\mathbf{w}(s) = \mathrm{d}\mathbf{u}(s)/\mathrm{d}s$. The position of the corresponding point on the deformed chain is denoted $\tilde{\mathbf{r}}(\tilde{s})$ and is given by

$$\tilde{\mathbf{r}}(\tilde{s}) = \mathbf{E}\cdot\mathbf{r}(s) \tag{3}$$

Points on the deformed contour are parameterized by the distance $\tilde{s}$ measured from one end of the polymer along the deformed path, where $\tilde{s}(s)$ is a nontrivial function of the position s of the corresponding point on the undeformed contour. Infinitesimal distances $\mathrm{d}\tilde{s}$ and $\mathrm{d}s$ at corresponding points on the deformed and undeformed contours are related by $\mathrm{d}\tilde{s}(s)/\mathrm{d}s = |\mathbf{E}\cdot\mathbf{u}(s)|$, which guarantees that $|\mathrm{d}\tilde{\mathbf{r}}(\tilde{s})/\mathrm{d}\tilde{s}| = 1$. The unit tangent vector and curvature of a given segment of the deformed contour are denoted by $\tilde{\mathbf{u}} \equiv \mathrm{d}\tilde{\mathbf{r}}/\mathrm{d}\tilde{s}$, and $\tilde{\mathbf{w}} \equiv \mathrm{d}\tilde{\mathbf{u}}/\mathrm{d}\tilde{s}$ and are related to the tangent vector $\mathbf{u}$ and curvature $\mathbf{w}$ of the corresponding segment of the undeformed contour by

$$\tilde{\mathbf{u}} = \mathbf{E}\cdot\mathbf{u}/|\mathbf{E}\cdot\mathbf{u}| \tag{4}$$

$$\tilde{\mathbf{w}} = \tilde{\mathbf{P}}\cdot\mathbf{E}\cdot\mathbf{w}/|\mathbf{E}\cdot\mathbf{u}|^2 \tag{5}$$

where $\tilde{\mathbf{P}} \equiv \boldsymbol{\delta} - \tilde{\mathbf{u}}\tilde{\mathbf{u}}$ is a projection operator for the plane perpendicular to $\tilde{\mathbf{u}}$.

As in the DE model, we assume that this affine deformation of the tube conformation is accompanied by a tangential contraction of the polymer along the tube, so as to maintain the length of the primitive chain. The effect of this contraction is (for sufficiently long polymers) to evacuate all but a fraction $1/\alpha(\mathbf{E})$ of the affinely deformed tube of each polymer, where

$$\alpha(\mathbf{E}) \equiv \int \frac{\mathrm{d}\mathbf{u}}{4\pi} |\mathbf{E}\cdot\mathbf{u}| \tag{6}$$

is the average fractional extension of the tube.

Using eqs 4−6, together with eqs I.17−I.18 for the equilibrium values of the probability distributions $f(\mathbf{u}', s) = \langle\delta[\mathbf{u}' - \mathbf{u}(s)]\rangle$ and $\mathbf{F}(\mathbf{u}', s) = \langle\mathbf{w}(s)\mathbf{w}(s)\delta[\mathbf{u}' - \mathbf{u}(s)]\rangle$, it is straightforward to show that the values of f and $\mathbf{F}$ obtained immediately after a step deformation of an ensemble of chains with $L \gg L_{\text{p}}$ are given by

$$f(\mathbf{u}', \mathbf{E}) \equiv \int \frac{\mathrm{d}\mathbf{u}}{4\pi\alpha(\mathbf{E})} |\mathbf{E}\cdot\mathbf{u}|\, \delta(\tilde{\mathbf{u}} - \mathbf{u}') \tag{7}$$

$$\mathbf{F}(\mathbf{u}', \mathbf{E}) \equiv \frac{1}{L_{\text{p}}L_{\text{e}}} \int \frac{\mathrm{d}\mathbf{u}}{4\pi\alpha(\mathbf{E})} \frac{\tilde{\mathbf{P}}\cdot\mathbf{B}\cdot\tilde{\mathbf{P}}}{|\mathbf{E}\cdot\mathbf{u}|^3} \delta(\tilde{\mathbf{u}} - \mathbf{u}') \tag{8}$$

where $\mathbf{B} \equiv \mathbf{E}\cdot\mathbf{E}^T$ is the Finger strain, L_{e} is the entanglement length, and $\tilde{\mathbf{u}}(\mathbf{u})$ is given by eq 4.

Using eq I.35 for $\boldsymbol{\sigma}_{\text{curve}}$, the curvature stress obtained immediately after a deformation may be expressed as a sum

$$\boldsymbol{\sigma}_{\text{curve}}(\mathbf{E}) = \frac{\rho T}{L_{\text{e}}} [\mathbf{Q}_{\text{bend}}(\mathbf{E}) + \mathbf{Q}_{\text{link}}(\mathbf{E})] \tag{9}$$

in which

$$\mathbf{Q}_{\text{bend}}(\mathbf{E}) \equiv L_{\text{p}}L_{\text{e}}\langle\tilde{\mathbf{w}}\tilde{\mathbf{w}} - |\tilde{\mathbf{w}}|^2\tilde{\mathbf{u}}\tilde{\mathbf{u}}\rangle$$

$$\mathbf{Q}_{\text{link}}(\mathbf{E}) \equiv \langle 3\tilde{\mathbf{u}}\tilde{\mathbf{u}} - \boldsymbol{\delta}\rangle \tag{10}$$

are contributions per entanglement length, in units of thermal energy T, to the bending stress $\boldsymbol{\sigma}_{\text{bend}}$ and link stress $\boldsymbol{\sigma}_{\text{link}}$ defined in eq I.27. The use of eqs 7 and 8 to evaluate the averages yields

$$\mathbf{Q}_{\text{bend}}(\mathbf{E}) = \int \frac{\mathrm{d}\mathbf{u}}{4\pi\alpha(\mathbf{E})} \frac{\tilde{\mathbf{P}}\cdot\mathbf{B}\cdot\tilde{\mathbf{P}} - \tilde{\mathbf{u}}\tilde{\mathbf{u}}(\tilde{\mathbf{P}}:\mathbf{B})}{|\mathbf{E}\cdot\mathbf{u}|^3} \tag{11}$$

$$\mathbf{Q}_{\text{link}}(\mathbf{E}) = \int \frac{\mathrm{d}\mathbf{u}}{4\pi\alpha(\mathbf{E})} |\mathbf{E}\cdot\mathbf{u}|(3\tilde{\mathbf{u}}\tilde{\mathbf{u}} - \boldsymbol{\delta}) \tag{12}$$

For comparison, the corresponding result of the DE model of flexible chains is

$$\boldsymbol{\sigma}_{\text{coil}}(\mathbf{E}) = \frac{\rho T}{L_{\text{e}}} \mathbf{Q}_{\text{link}}(\mathbf{E}) \tag{13}$$

where L_{e} is the entanglement contour length in a fluid of flexible or loosely-entangled chains.

The magnitude of the differences between the stresses predicted by the present model and the DE model provides a measure of the extent to which the present model predicts violations of the stress optic relation, since the predicted optical birefringence in either tube model is proportional to $\mathbf{Q}_{\text{link}}$ and thus is proportional to the elastic stress of the DE model.

A. Uniaxial Extension. We first consider the case of uniaxial extension by a factor of λ along the z direction, with a deformation tensor

$$\mathbf{E} = \begin{pmatrix} \lambda^{-1/2} & 0 & 0 \\ 0 & \lambda^{-1/2} & 0 \\ 0 & 0 & \lambda \end{pmatrix} \tag{14}$$

for which we calculate the tensile stress

$$\sigma_T(\lambda) = \sigma_{zz}(\mathbf{E}) - \sigma_{xx}(\mathbf{E}) \tag{15}$$

obtained immediately after deformation.

Plots of tensile stress obtained from both the worm-like chain model considered here and the DE model are shown in Figure 1. Results for both models were obtained by numerical evaluation of the integrals in eqs 11 and 12. For $\lambda - 1 \ll 1$, both models give $\sigma_T(\lambda) \simeq 3G(0)(\lambda - 1)$, as required by linear response theory. In the strongly nonlinear region $\lambda \gg 1$, the worm-like chain model is found to give tensile stress that continues to rise linearly with λ, though with a slightly smaller slope than that found in the linear regime. In contrast, the DE model predicts a rapid approach to a finite limiting value of $\sigma_T(\lambda)$, of order the plateau modulus $G(0)$, which is the limiting value obtained from $\boldsymbol{\sigma}_{\text{coil}}$ when all of the links are oriented exactly parallel to the axis of extension.

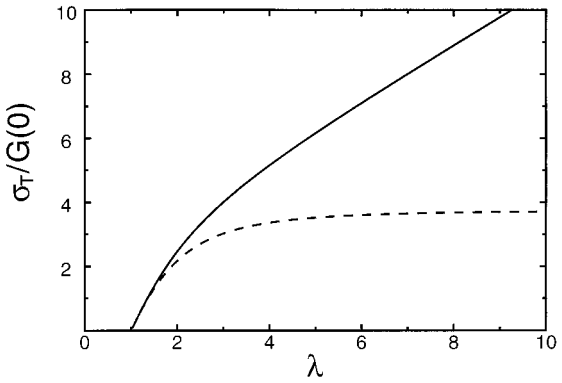

Figure 1. Plot of tensile stress $\sigma_T(\lambda)$ for long chains under uniaxial extension, as a function of the ratio λ of deformed to undeformed length, with stress measured in units of the plateau modulus $G(0)$. The solid line is the prediction of the worm-like chain model and dashed line is that of the DE flexible chain model.

The mathematical origin of the unbounded increase in σ_T with increasing λ in the worm-like chain model may be understood by considering the asymptotic behavior of the integral in eq 11 for $\mathbf{Q}_{\text{bend}}(\lambda)$ in the limit of large λ, since $\mathbf{Q}_{\text{bend}}(\lambda)$ is found to dominate $\boldsymbol{\sigma}_{\text{curve}}$ in this limit. It is found that this integral is dominated by the contributions of segments whose initial orientations are very close to the $x-y$ plane, which yield the smallest values for the ratio

$$|\mathbf{E}\cdot\mathbf{u}| = \sqrt{\lambda^2 \cos^2(\theta) + {}^1/_\lambda \sin^2(\theta)} \tag{16}$$

of the deformed to the undeformed segment length, in which $\cos(\theta) \equiv \mathbf{u}\cdot\hat{\mathbf{z}}$. These are the segments of chain that form hairpins in the deformed chain conformation, as shown schematically in Figure 2. While the average extension $\alpha(\mathbf{E})$ for randomly oriented segments is of order λ for $\lambda \gg 1$,, segments with orientations $\theta \simeq {}^\pi/_2$ are contracted by a factor $|\mathbf{E}\cdot\mathbf{u}| \simeq \lambda^{-1/2}$. This contraction of the chain length, along with the stretching of $\mathbf{w}$ in the z direction leads to root-mean-square values of $\tilde{w}_z$ for such segments that are larger than those typical of the equilibrium state by factors of order λ^2. The fraction of the contour length of the deformed chain that is comprised of such tightly curved segments may be estimated to be of order λ^{-3} by noting that (i) such large curvatures are produced only by a small population of segments whose initial orientation lies within a range of angles $|\theta - {}^\pi/_2| \lesssim \lambda^{-3/2}$ of the $x-y$ plane and (ii) the contribution of these segments to the length of the deformed chain is further reduced by a factor of order $\lambda^{3/2}$ due to the fact that the segments of interest are contracted by a factor $|\mathbf{E}\cdot\mathbf{u}| \simeq \lambda^{-1/2}$ while the average extension $\alpha(\mathbf{E})$ of a randomly oriented segment is of order λ. Multiplying a large factor of $\tilde{w}_z\tilde{w}_z \approx \lambda^4$, for the mean-squared curvature within such a tightly curved tube segment, by a factor of order λ^{-3}, for the fraction of the contour length occupied by such regions of high curvature, we thus obtain a stress component σ_{zz} of order λ, as found above by numerical integration.

Qualitatively, the above analysis indicates that for $\lambda \gg 1$ the tensile stress in the worm-like chain model is dominated by the contribution of the hairpins, i.e., the contributions of rare segments of chain along which the curvature is much higher than that obtained in the equilibrium state (although the curvature of most chain segments is suppressed rather than enhanced by deformation), along which the chain is oriented relatively close to the $x-y$ plane (although most of the deformed chain is instead aligned nearly parallel to the z axis), which make up only a small fraction of the deformed contour length.

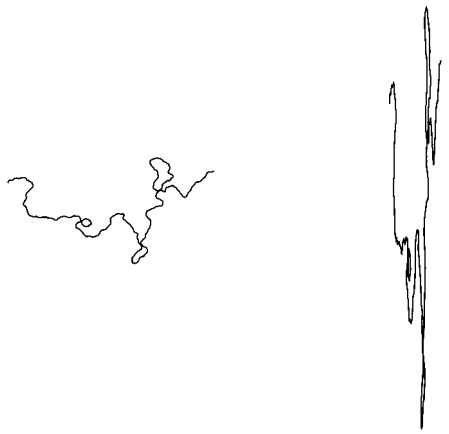

Figure 2. Typical conformations of a computer generated two-dimensional (2D) worm-like chain before (left) and after (right) a 2D affine uniaxal extension along the $\hat{\mathbf{z}}$ (vertical) direction, for $\lambda = 4$, without the retraction that would be required to maintain a constant contour length. The deformed conformation consists of long oriented segments separated by occasional deformation-induced hairpins.

B. Simple Shear. We now consider the response to a sudden shear deformation with a total shear strain γ, with a deformation tensor

$$\mathbf{E} = \begin{pmatrix} 1 & \gamma & 0 \\ 0 & 1 & 0 \\ 0 & 0 & 1 \end{pmatrix} \tag{17}$$

for which we calculate the shear stress and the first and second normal stresses

$$\sigma_{xy}(\gamma) \equiv \sigma_{xy}(\mathbf{E})$$

$$N_1(\gamma) \equiv \sigma_{xx}(\mathbf{E}) - \sigma_{yy}(\mathbf{E})$$

$$N_2(\gamma) \equiv \sigma_{yy}(\mathbf{E}) - \sigma_{zz}(\mathbf{E}) \tag{18}$$

obtained immediately after deformation. The calculated normal stress $N_1(\gamma)$ and shear stress $\sigma_{xy}(\gamma)$ are found, within numerical accuracy, to obey the Lodge−Meissner relation[16]

$$N_1(\gamma) = \sigma_{xy}(\gamma)\gamma \tag{19}$$

which is known to be a general consequence of frame invariance.[17]

The values for the shear stress $\sigma_{xy}(\gamma)$ and first normal stress $N_1(\gamma)$ obtained from both the worm-like chain model considered here and from the DE model of flexible chains are shown in Figure 3. Both models are found to exhibit some degree of strain softening, in that the

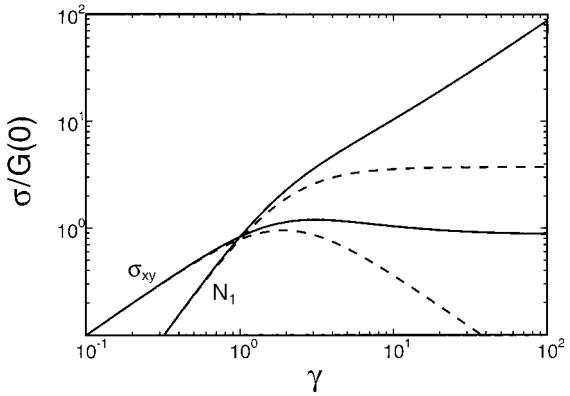

Figure 3. Plot of shear stress $\sigma_{xy}(\gamma)$ and first normal stress $N_1(\gamma)$ for long chains under step shear, with stress in units of the plateau modulus $G(0)$. Solid lines are the predictions of the worm-like chain model and dashed lines those of the DE flexible chain model.

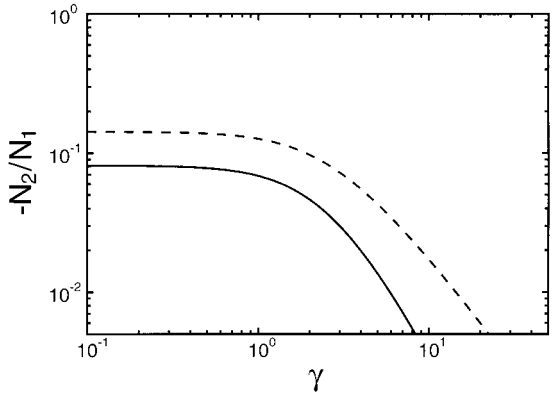

Figure 4. Ratio $-N_2(\gamma)/N_1(\gamma)$ of second and first normal stress for simple step shear. Solid line is the result of the worm-like chain model and dashed line that of the DE flexible chain model.

nonlinear modulus $G(\gamma) \equiv \sigma_{xy}(\gamma)/\gamma$ is found to decrease with γ, but the predicted degree of softening is much less for the present worm-like chain model than for the DE model: At large values of γ, the present model predicts that $\sigma_{xy}(\gamma)$ approaches a constant asymptotic value of order the plateau modulus, whereas the DE model predicts a shear stress that decreases as γ^{-1} in this limit. Correspondingly, $N_1(\gamma)$ rises linearly with γ for $\gamma \gg 1$ in the worm-like chain model but approaches a finite asymptotic value of order the plateau modulus in the DE model.

The appearance of a well-defined maximum in $\sigma_{xy}(\gamma)$ in the DE model implies the existence of a mechanical instability towards shear banding in systems undergoing large step shears, which is closely related to the corresponding prediction of an instability in fast steady shear flow. The shear stress for the present model also shows a maximum at a value of $\gamma \simeq 3$, visible in Figure 3, although with a maximum shear stress only about 30% higher than the asymptotic value obtained for $\gamma \gg 1$. The present model therefore also predicts a mechanical instability in large step shears, although the driving force for the instability is much weaker than in the DE model and thus is presumably more susceptible to both inaccuracies in the model and kinetic limitations.

The second normal stress $N_2(\gamma)$ is, as in the DE model, negative in sign and smaller in magnitude than the first normal stress. The ratio $N_2(\gamma)/N_1(\gamma)$, which is shown in Figure 4, approaches an asymptotic value of

$$\lim_{\gamma \to 0} \frac{N_2(\gamma)}{N_1(\gamma)} = -\frac{4}{49} \simeq -0.082 \qquad (20)$$

in the limit of small γ. This may be compared to the value of $N_2/N_1 = -1/7 = -0.143$ predicted by the DE model, which is in reasonable agreeement with most available data on flexible polymer systems.

The asymptotic behavior of $N_1(\gamma)$ and $\sigma_{xy}(\gamma)$ at large values of γ may be understood by again considering the integral defining $\mathbf{Q}_{\text{bend}}$, since $\mathbf{Q}_{\text{bend}}$ is found to dominate $\boldsymbol{\sigma}_{\text{curve}}$ in this limit. For this purpose, we estimate the xx element of $\mathbf{Q}_{\text{bend}}$, which is found to dominate $N_1(\gamma)$, and rely on the Lodge−Meissner relation to relate $N_1(\gamma)$ to $\sigma_{xy}(\gamma)$. Equation 11 for $\mathbf{Q}_{\text{bend}}$ is dominated (as for uniaxial extensional) by the contributions of chain segments with orientations near those for which the fractional extension

$$|\mathbf{E}\cdot\mathbf{u}| = \sqrt{1 + 2\gamma u_x u_y + \gamma^2 u_y^2} \qquad (21)$$

takes on its minimum possible value. In the case of shear deformations, a minimum value of $|\mathbf{E}\cdot\mathbf{u}| \simeq \gamma^{-1}$ is obtained for chain segments with initial orientations for which $u_z = 0$ and $u_y/u_x \simeq -1/\gamma$, which are rotated into final orientations $\tilde{\mathbf{u}}$ that are nearly parallel to the y axis. For such segments, it is straightforward to show that the root-mean-squared value of $\tilde{w}_x$ in the deformed state is larger than that typical of the equilibrium state by a factor of order γ^3. The fraction of the chain over which the curvature is so large may be shown to be of order $1/\gamma^5$ by noting that (i) the dominant contribution to σ_{xx} in eq 11 arises from segments with a range of initial orientations with an angular width $\Delta\phi \propto 1/\gamma^2$ and $\Delta\theta \propto 1/\gamma$, where $\cos(\theta) = u_z$ and $\tan(\phi) = u_y/u_x$, giving a reduction in their contribution to N_1 by a factor of $1/\gamma^3$, and (ii) the segments in question are actually contracted by a factor of $|\mathbf{E}\cdot\mathbf{u}| \simeq \gamma^{-1}$, whereas the average extension $\alpha(\mathbf{E})$ of a randomly oriented segment is of order γ, thus further reducing the contribution of such segments by a factor of order γ^{-2}. Multiplying these factors yields a dominant contribution to $\sigma_{xx}(\gamma) \simeq N_1(\gamma)$ of order γ, as obtained above by numerical integration.

Qualitatively, the dominant contributions to $N_1(\gamma)$ are thus again found to be those of hairpins, i.e., highly curved segments of chain along which the orientation varies significantly from the flow direction. More specifically, the stress obtained after a step shear is apparently dominated by a subset of hairpins along which the deformed chain is oriented near the y (i.e., velocity-gradient) axis.

III. Continuous Flows

We now consider the response to continuous flows, that is, flow histories in which the velocity gradient tensor $\kappa \equiv (\nabla\mathbf{v})^T$ remains finite and varies continuously at all times. We will further restrict ourselves to flows in which the scalar rate of deformation κ always remains less than the lowest relaxation rate for the tension stress σ_{tens}, so that the primitive chain may be treated as effectively inextensible. In this limit, the tension $\mathcal{T}(s, t)$ may be treated as a Lagrange multiplier field whose value must chosen so as to prevent local extension or compression of the chain, and the stress may be expressed as a sum of "elastic" curvature and orienta-

tional contributions that respond comparatively slowly to changes in $\kappa(t)$, and a "viscous" tension contribution that responds essentially instantaneously. The elastic stresses are expected to dominate the total over a range of deformation rates extending far into the non-Newtonian regime, and so we will again focus primarily upon calculating elastic stresses. Subsections A and B contain discussions of the response of the elastic stress $\boldsymbol{\sigma}_{\text{curve}} + \boldsymbol{\sigma}_{\text{orient}}$ in the limits of, respectively, coil-like and rod-like chains. Subsection C contains a brief discussion of the viscous contribution $\boldsymbol{\sigma}_{\text{tens}}$.

A. Coil-like Polymers: $L \gg L_p$. In the limit of coil-like polymers, with $L \gg L_p$, we may ignore the orientational stress and approximate the total elastic stress by σ_{curve}. In a fluid subjected to steady deformation with a characteristic scalar deformation rate κ, the curvature stress is expected to exhibit three regimes of dynamical behavior:

1. At deformation rates $\kappa \ll \tau_{\text{rep}}^{-1}$, there is a linear viscoelastic regime in which the distribution of polymer conformations is only weakly deformed from its equilibrium state.

2. At deformation rates $\tau_{\text{rep}}^{-1} \ll \kappa \ll \tau_{\text{end}}^{-1}$, there is a moderately nonlinear regime in which the time κ^{-1} needed to substantially deform the polymer conformation becomes much shorter than the time $\tau_{\text{rep}} \propto L^2/D$ necessary to disengage the chain from the tube but remains much longer than the time $\tau_{\text{end}} \propto L_p^2/D$ necessary to randomize the direction of the end of the chain by diffusing a single persistence length along the chain contour. In this regime, we thus expect the distribution of segment orientations to be strongly anisotropic near the center of the chain but almost isotropic at the chain ends.

3. At deformation rates $\kappa \gg \tau_{\text{end}}^{-1}$, there exists a strongly nonlinear regime in which the distribution of orientations must become strongly anistropic even at ends of the chain.

The mechanisms of stress buildup and stress relaxation in a tube model of semiflexible chains are similar to those operative in the DE model of flexible chains: Sections of tube are created at the tube ends and diffuse along the chain by reptation until they are destroyed again at the chain ends. In regimes 1 and 2, the distribution of initial orientations of new segments created at the chain ends is nearly isotropic, as in the DE model, while in regime 3, it becomes anisotropic.

A reasonable approximation for the curvature stress in regimes 1 and 2 may thus be obtained, following reasoning nearly identical to that used in constructing the DE model, from a Kaye−Berstein-Kearsley-Zapas (K-BKZ)[18] integral approximation

$$\boldsymbol{\sigma}_{\text{curve}}(t) = \int_{-\infty}^{t} \mathrm{d}t' \, \frac{\partial \bar{\chi}(t - t')}{\partial t'} \, \boldsymbol{\sigma}_{\text{curve}}(\mathbf{E}(t, t')) \quad (22)$$

In the above, $\boldsymbol{\sigma}_{\text{curve}}(\mathbf{E})$ is the curvature stress generated by a step deformation of total deformation $\mathbf{E}$; $\boldsymbol{E}(t, t')$ is the total deformation of a fluid element between times t' and t, which satisfies $\partial \mathbf{E}(t, t')/\partial t = \kappa(t) \cdot \mathbf{E}(t, t')$; and $\bar{\chi}(t - t')$ is the DE relaxation function used in eq 2. As in the DE model, we may interpret t' as the time at which a section of tube was created at either end of the chain and $\boldsymbol{\sigma}_{\text{curve}}(\mathbf{E}(t, t'))$ as being proportional to the average contribution to the stress at t, per surviving segment, from segments that were created at time t' and have survived to time t. This physical justification of eq 22 relies upon the assumption that the distribution of orientations of newly created segments at the chain ends remains isotropic, since our calculation of $\boldsymbol{\sigma}_{\text{curve}}(\mathbf{E})$ assumes an isotropic initial distribution of link orientation, and thus remains valid only in regimes 1 and 2.

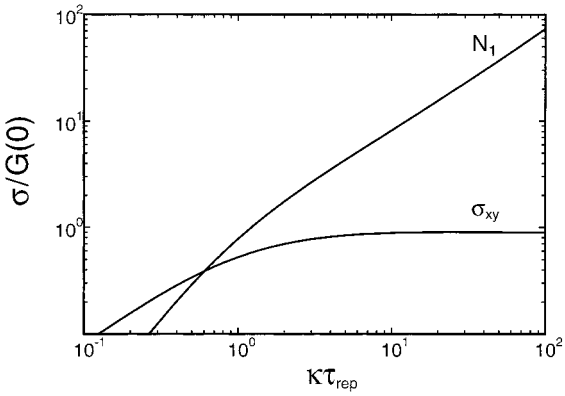

Figure 5. Shear stress $\sigma_{xy}(\kappa)$ and first normal stress $N_1(\kappa)$ for steady shear flow, with shear rate κ expressed in units of the disengagement time τ_{rep}, and stress in units of the plateau modulus $G(0)$.

Beyond the restriction to shear rates for which the chain ends remain randomly oriented, the further approximation implicit in our use of eq 22 lies in its approximate treatment of the continous tangential retraction of the ends of the polymer toward the center along the tube contour, which allows the polymer to maintain a fixed contour length. The effect of this tangential flow is taken into account in an approximate manner here, as in the DE model, by the inclusion of the factor of $1/\alpha(\mathbf{E})$ within eqs 11 and 12, which replaces the actual effects of tangential retraction by the average fractional retraction $1/\alpha(\mathbf{E})$ experienced during a corresponding step deformation. There is no obvious reason to expect this "preaveraging" of the effects of tangential retraction to cause substantially greater inaccuracies in the present tube model than in the original DE model, but the effects of the approximation are ultimately unknown.

Figure 5 shows numerical results for the shear stress $\sigma_{xy}(\kappa)$ and first normal stress $N_1(\kappa)$ obtained from eq 22 under conditions of steady shear flow with a shear rate κ, such that $\kappa_{ij} = \kappa \delta_{ix} \delta_{jy}$. The behavior of the stress as a function of reduced shear rate $\kappa\tau_{\text{rep}}$ is similar in most respects to that shown in Figure 3 for the stress obtained under step shear as a function of total strain γ: At shear rates $\kappa\tau_{\text{rep}} \gg 1$, the worm-like chain model yields an asymptotic behavior

$$N_1(\kappa) \approx G(0)(\kappa\tau_{\text{rep}}) \quad (23)$$

$$\sigma_{xy}(\kappa) \approx G(0) \quad (24)$$

The DE model predicts much more drastic shear thinning, with $N_1(\kappa) \approx G(0)$ and $\sigma_{xy}(\kappa) \approx G(0)(\kappa\tau_{\text{rep}})^{-1/2}$, leading to a robust prediction of a flow instability. The K-BKZ approximation for the worm-like chain model instead predicts a (barely) stable steady shear flow at large shear rates, since there is no apparent maximum in $\sigma_{xy}(\kappa)$ in Figure 5, despite the prediction of a weak mechanical instability for large step shear deformations.

In the appendix, we derive (but do not solve) a set of rigorous differential constitutive relations for long, tightly-entangled chains, which can in principle yield an accurate description of the effects of tangential flow.

This differential constitutive relation is a direct extension of one derived (but not solved) by DE to describe entangled flexible chains.[3]

B. Rod-like Polymers: $L \ll L_p$. In the limit $L \ll L_p$ of rod-like polymers, we expect three regimes of deformation rate:

1. At deformation rates $\kappa \ll \tau_{rod}^{-1}$, the system may be described by linear viscoelasticity.

2. At deformation rates, $\tau_{rod}^{-1} \ll \kappa \ll \tau_{rep}^{-1}$, the time scale κ^{-1} becomes smaller than the rotational diffusion time τ_{rod} but remains larger than the reptation time τ_{rep}, yielding a weakly nonlinear regime in which the distribution of orientations becomes strongly anisotropic but in which the fluctuations of the polymers' internal bending modes are only weakly perturbed.

3. At deformation rates $\kappa \gg \tau_{rep}^{-1}$, one expects a strongly nonlinear regime in which the deformation becomes rapid enough to significantly perturb the fluctuations of bending modes.

A tractable approximate description may be constructed for regimes 1 and 2. In the limit $L \ll L_p$ of interest, where $\mathbf{u}(s)$ must become almost independent of s, we may approximate the orientational distribution function $f(\mathbf{u}, s, t)$ by its average $\bar{f}(\mathbf{u}, t) \equiv \int_0^L ds\, f(\mathbf{u}, s, t)/L$. By use of this approximation, it is then straightforward to show, by a direct extension of the reasoning used in (II) to describe the linear response of $\sigma_{orient}(t)$, that in regimes 1 and 2, $\bar{f}(\mathbf{u}, t)$ approximately obeys a Smoluchowski equation

$$\left[\frac{\partial}{\partial t} - D_{rod}\nabla^2\right]\bar{f} = -\frac{\partial}{\partial \mathbf{u}}\cdot(\mathbf{g}\bar{f}) \tag{25}$$

appropriate to an ensemble of rigid rods whose orientations are simultaneously being rotated by flow and diffusing, where $D_{rod} = D_{rep}/LL_p$ is the effective rotational diffusivity given in eq II.77, and $\mathbf{g} = (\boldsymbol{\delta} - \mathbf{uu})\cdot\boldsymbol{\kappa}\cdot\mathbf{u}$ is the value of $d\mathbf{u}/dt$ in the absence of rotational diffusion, as given previously in eq II.B4. The orientational stress $\boldsymbol{\sigma}_{orient}$ is thus expected to be identical to the stress

$$\boldsymbol{\sigma}_{orient}(t) = \frac{\rho T}{L}\int d\mathbf{u}\,(3\mathbf{uu} - \boldsymbol{\delta})\, f(\mathbf{u}, t) \tag{26}$$

obtained in a rigid rod model with the same value of D_{rod}. Within regimes 1 and 2, the Deborah number $\kappa\tau_{rep}$ relevant to $\boldsymbol{\sigma}_{curve}$ remains small, and so $\boldsymbol{\sigma}_{curve}$ may be approximated by the linear response expression

$$\boldsymbol{\sigma}_{curve}(t) = \frac{7}{5}\frac{T\rho}{L_e}\int_{-\infty}^{t} dt'\, \bar{\chi}(t - t')2\mathbf{D}(t') \tag{27}$$

where $2\mathbf{D}(t) = \boldsymbol{\kappa}(t) + \boldsymbol{\kappa}^T(t)$ and $\bar{\chi}(t - t')$ is the DE relaxation function defined in eq II.56. In regimes 1 and 2, the total elastic stress may thus reasonably be approximated by simply adding the results of a nonlinear treatment of the orientational stress of a rigid-rod model, calculated with an effective diffusivity $D_{rod} = D_{rep}/LL_p$, to a curvature contribution that is calculated in a linear reponse approximation. Numerical calculations of the non-Newtonian behavior of the rigid-rod model have been presented previously by many authors.[19]

In regime 3, both the linear response approximation for the curvature stress and the use of the linear response (i.e., equilibrium) expression for the rotational diffusivity D_{rod} are expected to fail.

C. Tension Stress. The tension stress in a system of inextensible chains may (like the viscous contribution to the stress in any system with rigid constraints[3]) be expressed as a product of the form

$$\boldsymbol{\sigma}_{tens}(t) = \boldsymbol{\eta}:\boldsymbol{\kappa}(t) \tag{28}$$

where $\boldsymbol{\eta}$ is a fourth-order viscosity tensor that depends upon the distribution of polymer conformations. To calculate $\boldsymbol{\eta}$, we combine eq I.37, which gives the tension stress as an integral $\boldsymbol{\sigma} = \rho/L \int_0^L ds\langle\mathcal{T}(s)\ \mathbf{u}(s)\mathbf{u}(s)\rangle$ (where $\mathcal{T}(s)$ is the distribution of tension along the chain), with eq II.B10, which gives $\mathcal{T}(s)$ for an affinely deforming inextensible chain as an integral $\mathcal{T}(s, t) = \zeta\int_0^L ds'\ K(s, s')\mathbf{u}(s')\mathbf{u}(s'):\boldsymbol{\kappa}$, where ζ is a coefficient of friction for tangential motion of the chain relative to the tube, and $K(s, s')$ is Green's function solution to $\partial^2K(s, s')/\partial s^2 = -\delta(s - s')$ with $K(s, s') = 0$ at $s = 0$ and L. Substitution for $\mathcal{T}(s)$ yields a stress of the form given in eq 28, with a viscosity tensor

$$\boldsymbol{\eta} = \frac{\rho\zeta}{L}\int_0^L ds\int_0^L ds'\ K(s, s')\,\langle\mathbf{u}(s)\mathbf{u}(s)\mathbf{u}(s')\mathbf{u}(s')\rangle \tag{29}$$

Green's function $K(s, s')$ is given explicitly in eq II.B13 as a function of the form $K(s, s') = L\hat{K}(x, x')$, where $x \equiv s/L$ and $x' = s'/L$, with $\hat{K}(x, x') = x\Theta(x' - x) + x'\Theta(x - x') - xx'$. Using this form for K, we may rewrite $\boldsymbol{\eta}$ as

$$\boldsymbol{\eta} = \frac{\rho T}{L}\frac{L^2}{D_{rep}}\int_0^1 dx\int_0^1 dx'\ \hat{K}(x, x')\,\langle\mathbf{u}(x)\mathbf{u}(x)\mathbf{u}(x')\mathbf{u}(x')\rangle \tag{30}$$

where we have re-expressed $\mathbf{u}$ as a function of x and used the Einstein relation $D_{rep} = T/(\zeta L)$ for the reptation diffusivity.

We use eq 30 here only to obtain order of magnitude estimates of $\boldsymbol{\eta}$ and $\boldsymbol{\sigma}_{tens}$. First, consider a steady shear or extensional flow with a scalar rate of deformation $\kappa \approx \tau_{rep}^{-1}$, near the crossover between Newtonian and non-Newtonian regimes of $\boldsymbol{\sigma}_{curve}$. Under these conditions, we expect the distribution of segment orientations to be moderately anisotropic, and the tensor $\langle\mathbf{u}(x)\mathbf{u}(x)\mathbf{u}(x')\mathbf{u}(x')\rangle:\boldsymbol{\kappa}$ to be on the order of κ for all values of x and x', giving a viscosity of order $\eta_{tens} \sim (\rho T/L)\tau_{rep}$ and a tension stress of order $\sigma_{tens} \approx \rho T/L$. Since this is smaller by a factor of L_e/L than the curvature stress $\sigma_{curve} \approx \rho T/L_e$ obtained at the same deformation rate, the tension stress will thus remain negligible for $\kappa \sim \tau_{rep}^{-1}$, as well as at all lower rates, whenever $L/L_e \gg 1$.

The behavior of $\boldsymbol{\sigma}_{tens}$ at deformation rates $\kappa \gg \tau_{rep}^{-1}$ is different for shear and extensional flow but is in either case similar to that found in the tube model of flexible chains as extended by Marrucci and Grizzuti[7] to take into account the effects of flow-induced tension. In extensional flow, segments of the tube become almost perfectly aligned along the axis of extension, and so $\langle\mathbf{u}(x)\mathbf{u}(x)\mathbf{u}(x')\mathbf{u}(x')\rangle:\boldsymbol{\kappa}$ is predicted to increase linearly with scalar rate of extension $\kappa \equiv d\ln(\lambda)/dt$. Since the curvature contribution to the tensile stress σ_T calculated in a K-BKZ approximation is expected to grow roughly exponentially with Weissenberg number $\kappa\tau_{rep}$ in this regime (corresponding to a linear growth with λ in a step deformation), $\boldsymbol{\sigma}_{tens}$ is thus predicted to remain small compared to $\boldsymbol{\sigma}_{curve}$ even at high Weissenberg numbers. In rapid steady shear flow, segments of the tube become almost perfectly aligned along the flow axis, with the

result, noted by Marrucci and Grizzuti, that $\langle \mathbf{u}(x)\mathbf{u}(x)\cdot\mathbf{u}(x')\mathbf{u}(x')\rangle:\kappa$ and $\boldsymbol{\sigma}_{tens}$ actually decrease with increasing shear rate at high shear rates. The tension stress is thus also predicted to remain small compared to $\boldsymbol{\sigma}_{curve}$ in very rapid shear flows.

IV. Limitations

The tube model considered above is a relatively simple one, closely analogous to the original DE tube model, whose validity may be limited as the result of any of several approximations made in its construction. Here, we comment on the expected consequences of several neglected effects.

A. Contour Length Fluctuations. In all of the above, we have taken the primitive chain to be essentially inextensible. A related approximation is made in the DE model, which ignores both the extensibility of the primitive chain and the contribution of flow-induced tension to the stress. The assumption of inextensibility is a much better approximation in the tightly-entangled regime of interest here than in the loosely-entangled regime to which the DE model applies. In the regime of interest, each chain is confined to a very narrow tube, so that the end-to-end length of a segment of the primitive chain can be subjected to only a very small fractional extension of its equilibrium length before the corresponding segment of polymer becomes fully extended. The resulting near inextensibility of the primitive chain is reflected in the large values found for the linear extension modulus B introduced in (I), which is the ratio of the tension induced in a chain segment to its fractional extension in the limit of small extensions, which was found to diverge as $B \approx TL_p/D_e^2$ in the limit of vanishing tube diameter D_e. These large values for B in turn lead to the very short relaxation times found in (II) for the relaxation of tension after an infinitesimal step deformation. The assumption of inextensibility adopted in this paper makes it impossible for us to describe the rapid transient responds of $\boldsymbol{\sigma}_{tens}(t)$ at very short times after a step deformation, but is by itself expected to have little effect upon the validity of predictions for the response to flow histories involving large but slowly varying rates of deformation or for the relaxation of stress at long times after a step deformation.

B. Constraint Release. A second approximation that this model shares with the DE model is the neglect of constraint release. The neglect of flow-induced constraint release is now believed[13,14] to be the most likely reason for the prediction by the DE model of much too drastic shear thinning in rapid steady shear flows and for the corresponding incorrect prediction of a flow instability. The original DE model predicts a vanishing shear stress in very rapid steady shear flow, as the result of the tendency of the deformation to cause nearly perfect alignment of segments of the primitive chain along the flow axis at high shear rates. Modification of the DE model to include the convective constraint release (CCR) mechanism identified by Ianniruberto and Marrucci[13] qualitatively changes the predictions of the tube model for rapid deformations, by introducing a relaxation mechanism with a rate of relaxation that increases linearly with deformation rate, and leads to the prediction for entangled flexible chains of a stress plateau at moderate shear rates (between the inverse reptation and Rouse times) in which $\sigma_{xy} \approx N_1 \approx G(0)$.

It is less clear what will be the effects of constraint release in the tightly-entangled regime, but there are reasons to suspect that they will be less drastic than those predicted for the loosely-entangled regime. We may describe the effects of constraint release as a diffusive motion of the primitive chain, similar to the Brownian motion of an unentangled worm-like chain, that must be superimposed on the deterministic affine deformation that would occur in the absence of constraint release. We may describe the diffusive component of the motion of the primitive chain by assigning each undulation mode with a wavenumber q in the range $L_p^{-1} \ll q \ll L_e^{-1}$ a relaxation rate $\omega(q) \simeq \tau_{CR}(qL_e)^4$, where the τ_{CR} is the lifetime of a randomly chosen entanglement or constraint before it is destroyed by constraint release. This form for $\omega(q)$ is based upon the following assumptions: (i) the spectrum of relaxation rates should have the same dependence on q as that characterizing the Brownian motion of an unentangled worm-like chain, and (ii) modes of wavelength $qL_e \approx 1$, which may relax by removal of a single contraint per entanglement length, should exhibit a relaxation rate $\omega(q) \approx \tau_{CR}^{-1}$. When the primitive chain is subjected to an affine shear deformation with a shear rate κ, then this diffusive motion of the tube is expected to be effective in equilibrating undulation modes for which $\omega(q) \gtrsim \kappa$, or, equivalently, all modes with wavelengths less than a crossover wavelength

$$L_c \approx L_e(\kappa\tau_{CR})^{1/4} \tag{31}$$

while having little effect upon the nearly affine deformation of modes of wavelength greater than L_c. If, following Ianniruberto and Marrucci, we take the rate of destruction of entanglements at very high shear rates to be $\tau_{CR}^{-1} \sim \kappa S_{xy}$ for $\kappa\tau_{rep} \gg 1$, where $S_{ij} = \langle u_i u_j - \delta_{ij}/3\rangle$ is a segment orientation tensor, then we find a crossover wavelength $L_c \sim L_e S_{xy}^{1/4}$. Because S_{xy} is never greater than unity and because the above reasoning become meaningless if L_c drops substantially below L_e, we can conclude from this result only that CCR leads to diffusive relaxation of modes with wavelengths comparable to L_e while having little effect on longer wavelength modes. Applying similar reasoning to the loosely-entangled case, by assuming a Rouse-like relaxation with $\omega(q) \propto q^2$, leads to a crossover length $L_c \sim L_e S_{xy}^{1/2}$ and then to the same qualitative conclusion: CCR strongly enhances the relaxation of modes with wavelengths up to about the entanglement length.

How effective this diffusive relaxation of short-wavelength modes is in randomizing segment orientations depends, however, upon the relative magnitudes of L_e and L_p. In the loosely-entangled regime, the orientations of consecutive entanglement segments of a single primitive chain are uncorrelated, so that entanglement length L_e and persistence length L_p of the primitive chain are essentially equal. In this regime, relaxation of modes with wavelengths up to L_e is sufficient to significantly randomize the distribution of segment orientations. In the tightly-entangled regime of interest here, where $L_e \ll L_p$, so that the orientations of neighboring entanglement segments are strongly correlated, the relaxation of modes with wavelength $q^{-1} \approx L_e \ll L_p$ is expected to lead only to a partial relaxation of the curvature of the chain, which might be described by a slight (i.e., order unity) dilation of the effective tube diameter. As long as the crossover length L_c remains much smaller than the range of orientational correlations along the polymer backbone, however, the relaxation of short-wavelength

bending modes is expected to have little effect upon the distribution of segment orientations. In the tightly-entangled regime, we expect $L_c \approx L_e$ to remain much less than the range of orientational correlations at the boundary between the linear and nonlinear rheological regimes, where $\kappa\tau_{rep} \approx 1$ and where the range of orientational correlations is still approximately L_p. This suggests that, in the tightly-entangled regime, there must exist some range of deformation rates extending into the nonlinear regime $\kappa\tau_{rep} \gtrsim 1$ in which convective constraint leads only to an order unity increase in the effective entanglement length and to a corresponding quantitative decrease in the magnitude of the stress, without causing any qualitative changes in the prediction of the simple reptation model.

C. Nonaffine Deformation. The above calculations have assumed a perfectly affine deformation of the tube. Since affine deformation is found to lead to large deformations in the formation of very tightly curved segments of tube, we must ask how tight the resulting hairpins can become and thus how large a deformation may be described, before the assumption of affine deformation becomes unphysical. For simplicity, we will explicitly discuss only the case of a step deformation.

The most obvious criterion for the breakdown of this approximation is that the typical radius of curvature within a hairpin clearly should not be forced to drop below the tube diameter, D_e. A more stringent bound is obtained by requiring that the typical hairpin radius must also remain greater than the entanglement length L_e, which in the limit of interest is greater than D_e, since the "walls" of the imaginary tube are formed by a porous network of other chains, in which only a few (i.e., of order 1) other chains per entanglement length pass close enough to the confined chain to be available to help enforce the assumed affine deformation.

In uniaxial extension, we estimate in section II.A that the typical radius of curvature R within a hairpin is smaller by a factor of λ^{-2} than the typical curvature $1/(L_eL_p)^{1/2}$ in the equilibrium state, giving a radius $R \approx (L_eL_p)^{1/2}/\lambda^2$. Requiring that this radius remain larger than L_e restricts λ to values smaller than a maximum strain of order

$$\lambda \approx (L_p/L_e)^{1/4} \tag{32}$$

Similarly, the analysis given in section II.B suggests that in simple shear the typical size of a hairpin (or, more precisely, of the subset of hairpins that dominates the curvature stress) decreases as $R \approx (L_eL_p)^{1/2}/\gamma^3$, giving a maximum shear strain

$$\gamma \sim (L_p/L_e)^{1/6} \tag{33}$$

At strains much greater than these values, the rapid decrease in the number of hairpins with increasing strain, due to continuing retraction of the polymer within the tube, is expected to cause a rapid decrease in the contribution of $\boldsymbol{\sigma}_{bend}$ to the curvature stress, yielding total stresses lower than those calculated above and stronger strain softening under shear. Since the ratio L_p/L_e is only about 10 in the very tightly-entangled F-actin solutions discussed in (II) and since these systems thus far seem to provide the best example of a tightly-entangled solution, with the highest values for the ratio L_p/L_e, the above restriction on the minimum hairpin size is a serious one, and probably places more stringent restrictions on the applicability of the simple tube model than any arising from the neglect of contour length fluctuations or constraint release.

V. Discussion

In the above, we have described some nonlinear theological properties for a tube model in which the tube or primitive chain is semiflexible and in which curvature stress relaxes by reptation. A detailed treatment has been given only for the case of step deformation of a solution of very long chains.

Our treatment of step deformations is based upon a calculation of the curvature stress induced by an assumed affine deformation of a worm-like primitive chain. It is found that the curvature stress is dominated in the limit of large strains by contributions arising from the curvature of deformation-induced hairpins, i.e., very tightly curved segments of the deformed primitive chain that occupy only a small fraction of its total contour length. This qualitative conclusion is based upon an analysis of eq 11, in which the mechanical bending stress $\boldsymbol{\sigma}_{bend}$ is expressed as an integral over all possible initial orientations of a chain segment, whose integrand was found to be sharply peaked around specific values of the initial (i.e., undeformed) segment orientation for which (i) the segment's length is subsequently contracted by deformation, (ii) its orientation is rotated into a direction far from the direction of extension (for uniaxial extension) or flow (for shear), and (iii) its curvature is on average greatly amplified. The effect of flow upon such hairpin-forming segments is opposite to that experienced by segments with most other orientations, for which large deformations typically (i) extend the segment, (ii) rotate it to an orientation very near the axis of extension or flow, and (iii) suppress its curvature.

The model is found to respond to step deformations in a manner intermediate between that predicted by the DE model of flexible chains and by classical rubber elasticity or the upper convected Maxwell (UCM) model. In shear deformations, the shear stress is predicted to approach a constant at large strains, rather than decreasing as γ^{-1} as in the DE model or increasing as γ as in the UCM model. This constitutes strain softening behavior, insofar as it yields a nonlinear modulus $G(t, \gamma) \equiv \sigma_{xy}(t, \gamma)/\gamma$ that decreases monotonically with increasing γ. In extension, the tensile stress is found to increase linearly with total elongation λ, rather than approaching a constant as in the DE model or increasing as λ^2 as in the UCM model.[17] The predicted behavior may be understood as the result of a nontrivial competition between the tendency of deformation to rapidly concentrate curvature within hairpins, yielding a large contribution to the stress per unit chain length, and a partially compensating tendency to decrease the fraction of the polymer contour length that is contained within hairpins.

Two simplifications that are common to this model and the DE model, the assumption of an inextensible primitive chain and the neglect of constraint release phenomena, are, it is argued, less important in the tightly-entangled regime of interest here than in the loosely-entangled regime that the DE model is intended to describe. The assumption of a perfectly affine deformation of the tube is, however, shown to become unphysical for sufficiently large deformations, because affine deformation would lead to unphysically large

values for the curvature within the hairpins that dominate the calculated stress. If the typical curvature within a hairpin were to stop increasing beyond some critical strain while the fraction of polymer contour length contained within hairpins continued to decrease with increasing strain, the dominant stress contribution arising from such hairpins might well begin to decrease with increasing strain. Relaxation of the assumption of affine deformation is thus expected, at sufficiently high strains, to lead to more strongly strain softening behavior than that predicted above and quite possibly to the reappearance of a pronounced maximum in the stress as a function of shear strain in step shear deformation, as well as to a corresponding mechanical instability. These speculations are, however, beyond the scope of the calculation actually presented above.

The strain softening behavior predicted here for tightly-entangled solutions of tangentially mobile chains stands (even after taking into account the various limitations of the model) in clear contrast to the strain hardening behavior expected for a cross-linked gel of tightly-entangled chains. We expect the stress in a system with cross-links between chains to be dominated by the tension stress and to exhibit strong strain hardening for reasons that were first discussed by MacKintosh et al.[15] Oscillatory shear experiments with variable strain magnitudes on F-actin solutions by Janmey and coworkers,[20,21] on samples which exhibit plateau moduli orders of magnitude larger than those found by other groups, have shown hardening of the apparent storage modulus at strains of a few percent. Similar measurements by Xu et al.[22] on F-actin samples with much smaller plateau moduli show weak strain thinning. These observations are consistent with the conclusion given in (II), that the linear viscoelastic properties of the high modulus samples studied by Janmey et al.[20,21] are closer to those expected for a lightly cross-linked gel than those predicted for a physically entangled solution. This conclusion is consistent with the results of a study documenting the extreme sensitivity of the elasticity of F-actin solutions to differences in preparation and storage conditions and a more recent report by Tang et al.[24] that reports chemical evidence of cross-linking in the high-modulus F-actin samples, apparently due to the formation of disulfide bonds between actin monomers. Measurements of nonlinear rheological behavior might thus provide a sensitive test of whether other samples of such tightly-entangled solutions of worm-like biopolymers are chemically cross-linked or only physically entangled, when (as was the case for F-actin) this information is difficult to obtain by other means.

Acknowledgment. The author acknowledges the financial support of the Exxon Education Foundation.

Appendix

Rigorous Constitutive Relations for $L \gg L_p$. We now derive a set of differential equations for the functions $f(\mathbf{u}, s, t)$ and $\mathbf{F}(\mathbf{u}, s, t)$, from which the elastic stress contributions may be calculated, which is asymptotically exact in the limit of very long chains, $L \gg L_p$. These equations are a straighforward generalization of those given for $f(\mathbf{u}, s, t)$ in section 7.9 of the monograph by Doi and Edwards.[3]

Our starting point is eqs II.B7 and II.B8 for the time derivatives of $f(\mathbf{u}, s, t)$ and $\mathbf{F}(\mathbf{u}, s, t)$. These equations cannot, in their present form, be used as the basis of an explicit calculation of f or $\mathbf{F}$ because each equation contains a term (the last on the right-hand side of each) involving an average of $\bar{\nu}(s)$, which cannot in general be re-expressed as functional of f or $\mathbf{F}$. To simplify terms involving $\bar{\nu}(s)$, we will assume in what follows that, in the limit of sufficiently long chains, we may ignore correlations in the orientations of widely separated points along the chain.

We first review Doi and Edward's derivation of a set of explicit equations for f and then extend the result to obtain a corresponding equation for $\mathbf{F}$. To make the content of the troublesome last term in eq II.B7 for f explicit, we use eq II.B11 for $\bar{\nu}(s)$ to write this as an integral

$$\left\langle \bar{\nu}(s) \frac{\partial \hat{f}(\mathbf{u}, s)}{\partial s} \right\rangle = \int_0^L \mathrm{d}s' \frac{\partial K(s, s')}{\partial s} \times \kappa : \left\langle \mathbf{u}(s')\mathbf{u}(s') \frac{\partial \hat{f}(\mathbf{u}, s)}{\partial s} \right\rangle \quad \text{(A1)}$$

where $K(s, s')$ is Green's function as given in eq II.B13 and where $\hat{f}(\mathbf{u}', s) \equiv \delta(\mathbf{u}(s) - \mathbf{u}')$. The assumption that correlations between $\mathbf{u}(s)$ and $\mathbf{u}(s')$ drop off rapidly with $|s - s'|$ may be made precise by defining a tensor correlation function

$$\mathbf{C}(\mathbf{u}, s, s') \equiv \langle \mathbf{u}(s')\mathbf{u}(s')\hat{f}(\mathbf{u}, s)\rangle - \langle \mathbf{u}(s')\mathbf{u}(s')\rangle f(\mathbf{u}, s) \quad \text{(A2)}$$

We assume in what follows that $\mathbf{C}(\mathbf{u}, s, s')$ becomes small for $|s - s'|$ greater than some correlation length ξ, where $\xi \ll L$ and $\xi \approx L_p$ in equilibrium. We also assume that in this limit we may ignore end effects and thus express $\mathbf{C}(\mathbf{u}, s, s')$ as a function $\mathbf{C}(\mathbf{u}, |s - s'|)$, rather than as a function of s and s' separately. After expressing eq Al in terms of $\mathbf{C}(\mathbf{u}, s, s')$, we may integrate eq Al by parts and drop all contributions that vanish as $\xi/L \to 0$, to obtain an partial differential equation for f as

$$Lf = -\frac{\partial}{\partial \mathbf{u}} \cdot (\mathbf{g} f) + (\kappa : \mathbf{u}\mathbf{u})\, f + \frac{\partial}{\partial s}(\langle \bar{\nu} \rangle f) \quad \text{(A3)}$$

where $f = f(\mathbf{u}, s, t)$ and $\bar{\nu} = \bar{\nu}(s, t)$ and

$$L \equiv \frac{\partial}{\partial t} - D \frac{\partial^2}{\partial s^2} \quad \text{(A4)}$$

is a diffusion operator. The average tangential velocity $\langle \bar{\nu}(s) \rangle$ is easily calculated using differential eq II.B5 for $\bar{\nu}(s)$ and assuming symmetry between the two ends of the chain, to obtain

$$\langle \bar{\nu}(s) \rangle = -\int_{L/2}^{s} \mathrm{d}s' \, \langle \mathbf{u}(s')\mathbf{u}(s') \rangle : \kappa \quad \text{(A5)}$$

Equations A3 and A5 together define Doi and Edwards's rigorous differential relation for $f(\mathbf{u}, s, t)$. In the case of flexible chains and in regimes 1 and 2 or the present model, eq A3 must satisfy the boundary conditon $f(\mathbf{u}, s, t) = 1/4\pi$ at either chain end. More generally, for a semiflexible primitiven chain, eq A3 must satisfy the boundary condition given in eq II.50.

To apply essentially identical reasoning to eq II.B8 for $\mathbf{F}$, we assume that correlations between the quantities $\mathbf{u}(s')\mathbf{u}(s')$ and $\mathbf{w}(s)\mathbf{w}(s)\hat{f}(\mathbf{u}, s)$ are short-ranged and

thereby obtain a corresponding differential equation for $\mathbf{F}(\mathbf{u}, s, t)$ as

$$L\,\mathbf{F} = -\frac{\partial}{\partial \mathbf{u}}\cdot(\mathbf{g}\mathbf{F}) + \mathbf{G}\cdot\mathbf{F}^T + \mathbf{F}\cdot\mathbf{G}^T + (\kappa:\mathbf{u}\mathbf{u})\,\mathbf{F} + \frac{\partial}{\partial s}(\langle\bar{\nu}\rangle\mathbf{F}) \quad \text{(A6)}$$

which must be solved subject to boundary condition of eq II.49, where $\langle\bar{\nu}(s)\rangle$ is again given by eq A5.

Simultaneous solution of eqs A3, A5, and A6 would yield an approximation for the stress that is asymptotically exact in the limit of very long chains and that could be applied even in the strongly nonlinear regime. Without solving the equations, we may note that in regimes 1 and 2, where the chains ends may be taken to be randomly oriented, the solutions for $\boldsymbol{f}(\mathbf{u}, s, t)$ and $\langle\bar{\nu}(s)\rangle$ in the worm-like chain model will be numerically identical to those produced by the corresponding treatment of the DE model at the same Deborah number. Numerical solution of the equations for either the DE model or the slightly more complicated model presented here is possible but has not, to the author's knowledge, been attempted.

It should be noted that the modified integral expression for the stress proposed by DE at the end of section 7.9 of their monograph, which was obtained independently by Marrucci,[25] is not a correct solution of eq A3 with isotropic boundary conditions at the chain ends and thus is not, as suggested by Doi and Edwards, a solution of their rigorous differential constitutive equation. Both DE and Marriucci proposed an integral equation for $\mathbf{S}(s, t) \equiv \langle\mathbf{u}(s, t)\mathbf{u}(s, t) - \boldsymbol{\delta}/3\rangle$ as

$$\mathbf{S}(s, t) = \int_{-\infty}^{t} \mathrm{d}t' \frac{\partial\chi(s, t, t')}{\partial t'}\,\mathbf{Q}_{\mathrm{link}}(t, t') \quad \text{(A7)}$$

where $\mathbf{Q}_{\mathrm{link}}(t, t') = \mathbf{Q}_{\mathrm{link}}[\mathbf{E}(t, t')]$ is the value of $\mathbf{S}(s, t)$ immediately after a step deformation, which is given in eq 12, for a deformation $\mathbf{E}(t, t')$ equal to the total deformation of a fluid element between times t' and t, and where $\chi(s, t, t')$ is the solution of the differential equation

$$L\,\chi(s, t, t') = \langle\bar{\nu}(s)\rangle \frac{\partial\chi(s, t, t')}{\partial s} \quad \text{(A8)}$$

for $t \geq t'$, with an initial condition $\chi(s, t', t') = 1$. The corresponding expression for the full segment orientation distribution $f(\mathbf{u}, s, t)$ is

$$f(\mathbf{u}, s, t) = \int_{-\infty}^{t} \mathrm{d}t' \frac{\partial\chi(s, t, t')}{\partial t'}\,\tilde{f}(\mathbf{u}, t, t') \quad \text{(A9)}$$

where $\tilde{f}(\mathbf{u}, t, t') \equiv f(\mathbf{u}, \mathbf{E}(t, t'))$ is the orientational distribution obtained after a hypothetical step strain by a deformation $\mathbf{E}(t, t')$. By evaluating the time derivative of eq A9 and manipulating the result into a form as close as possible to that given in eq A3, we obtain

$$L\,f = -\frac{\partial}{\partial \mathbf{u}}\cdot(\mathbf{g}f) + (\kappa:\mathbf{u}\mathbf{u})\,f + \frac{\partial\langle\bar{\nu}\rangle}{\partial s}\,f - \int_{-\infty}^{t} \mathrm{d}t' \frac{\partial\chi(s, t, t')}{\partial t'}\,\tilde{f}(\mathbf{u}, t, t') \int \mathrm{d}\mathbf{u}'\,\tilde{f}(\mathbf{u}', t, t')\mathbf{u}'\mathbf{u}':\kappa$$

For eq A10 to be equivalent to eq A3, the term in the second line of eq A10 would have to be equivalent to the proposed integral expression for $-f(\mathbf{u}, s,t)\langle\mathbf{u}(s)\mathbf{u}(s)\rangle:\kappa$, which is given by

$$-f(\mathbf{u}, s, t) \int_{-\infty}^{t} \mathrm{d}t' \int \mathrm{d}\mathbf{u}' \frac{\partial\chi(s, t, t')}{\partial t'}\,\tilde{f}(\mathbf{u}', t, t')\mathbf{u}'\mathbf{u}':\kappa \quad \text{(A11)}$$

These two quantities are simply not equivalent.

It is, in part, the observation that eq A9 is not a solution to the differential constitutive equation that motivated the use of the simpler K-BKZ approximation in eq 22, since the K-BKZ approximation returns correct results for the step-deformation behavior and for the low shear rate limit of the ratio N_2/N_1, like the above approximation and unlike the independent alignment approximation, but is easier to implement than the above approximation.

References and Notes

(1) Morse, D. C. *Macromolecules* **1998**, *31*, 7030.
(2) Morse, D. C. *Macromolecules* **1998**, *31*, 7044.
(3) Doi, M.; Edwards, S. F. *The Theory of Polymer Dynamics*; Oxford University Press: London, 1986.
(4) Doi, M.; Edwards, S. F. *J. Chem. Soc. Faraday II* **1978**, *74*, 1789, 1802, 1818; **1979**, *75*, 38.
(5) Doi, M. *J. Polym. Sci., Polym Lett. Ed*. **1981**, *19*, 265; *J. Polym. Sci., Polym. Phys. Ed*. **1983**, *21*, 667.
(6) Rubinstein, M.; Helfand, E.; Pearson, D. S. *Macromolecules* **1987**, *20*, 822.
(7) Marrucci, G.; Grizzutti, N. *Gazz. Chim. Ital*. **1988**, *118*, 179.
(8) Pearson, D. S.; Herbolzheimer, E.; Grizzuti, N.;i Marrucci, G. *J. Polym. Sci., Polym. Phys. Ed* **1991**, *29*, 1589.
(9) Milner, S. T.; McLeish, T. C. B. *Phys. Rev. Lett*. **1998**, *81*, 725.
(10) Graessley, W. W. *Adv. Polym. Sci*. **1982**, *47*, 67.
(11) des Cloizeaux, J. *Europhys. Lett*. **1988**, *5*, 437; *Macromolecules* **1990**, *23*, 3392.
(12) Rubinstein, M.; Colby, R. H. *J. Chem. Phys*. **1988**, *89*, 5291.
(13) Marrucci, G. *J. Non-Newtonian Fluid Mech*. **1996**, *62*, 279. Ianniruberto, G.; Marrucci, G. *J. Non-Newtonian Fluid Mech*. **1996**, *65*, 241.
(14) Mead, D. W.; Larson, R. G.; Doi, M. *Macromolecules* **1998**, *31*, 7895.
(15) MacKintosh, F. C.; Janmey, P. A.; Kas, J. *Phys. Rev. Lett*. **1995**, *75*, 4425.
(16) Lodge, A. S.; Meissner, J. *Rheol. Acta* **1972**, *11*, 351. Lodge, A. S. *Rheol. Acta* **1975**, *14*, 664.
(17) Larson, R. *Consitutive Equations for Polymer Melts and Solutions*; Butterworth: Boston, 1988.
(18) Kaye, A. *Note No. 134*; College of Aeronautics: Cranford U.K., *1962* Berstein, B.; Kearsley, E.A.; Zapas, L. J. *Trans. Soc. Rheol*. **1963**, *7*, 391.
(19) Bird, R. B.; Curtiss, C.; Armstrong, R. C.; Hassager, O. *Dynamics of Polymeric Liquids*, Volume 2; Wiley-Interscience: NY, 1987; Chapter 7 and references therein.
(20) Janmey, P. A.; Hvidt, S.; Oster, G. F.; Lamb, J.; Stossel, T. P.; Harwig, J. H. *Nature* **1990**, *347*, 95.
(21) Janmey, P. A.; Hivdt, S.; Käs, J.; Lerche, D.; Maggs, A. C.; Sackmann, E.; Schliwa, M.; Stossel, T. P. *J. Biol. Chem*. **1994**, *269*, 32503.
(22) Xu, J.; Palmer, A.; Wirtz, D. *Macromolecules* **1998**, *31*, 6486.
(23) Xu, J.; Schwarz, W. H.; Käs, J. A.; Stossel, T.. P.; Janmey, P. A.; Pollard, T. D. *Biophys. J*. **1999**, *74*, 2731.
(24) Tang, J. X.; Janmey, P. A.; Stossel, T. P.; Ito, T. *Biophys. J*. **1999**, *76*, 2208.
(25) Marrucci, G. *J. Non-Newtonian Fluid Mech*. **1986**, *21*, 329.

MA970475J